[1]Y S Waghode,

[1]S Habibuddin,
[1]Bhagyashri B,

[1]T S Hibare,

[1]Rushikesh R G,

[2]R R Kalesh,

[1]V A Bambole

Monitoring the Size of CdSe Quantum Dots for Dye-Sensitized Solar Cell with Temperature Gradient

Abstract: - Novel reaction parameters for synthesizing CdSe Quantum Dots (QD's) of particle size of unit dimensions measured in nanometer is claimed herewith. The investigation systematically explored various sets of reaction conditions, in particular, the impact of reaction temperature, on the structural, morphological, optical, and other atomic scale properties of the CdSe QD's. Particle Size, as small as, 1 nm and with stability at ambient temperature could be easily obtained with βME as the capping agent. Characterization of, thus synthesized, CdSe QD's were done using XRD, UV-Visible spectroscopy, SEM, FTIR, HRTEM, EDX, and SAED techniques.The XRD results revealed that the size of the particles is between 2.4nm to 9nm and is in the cubic phase. SEM images clearly shows that the particle size increases with the increasing temperature. Further, HRTEM confirms the average particle size to be 3.6nm and smallest particle size as 1 nm. Also observed is intermixing of both, wurtzite and zinc blende structures. The EDX study confirms the percentage of Cd and Se to be 76.03 % and 23.96 % respectively. The comprehensive characterization techniques conduced collectively verify the successful synthesis of CdSe QDs. Furthermore, their size can be precisely regulated by altering the synthesis temperature.

The CdSe QD's nanoparticles remained stable in ambient conditions over longer period of time.

Keywords: Quantum Dots (QD's), Capping agents, Colloidal Method, Wurtzite Structure, Dye-Sensitized Solar Cell.

I. INTRODUCTION

Nanostructure material is 10^{-5} times smaller than a human hair's diameter; it is one billionth of a meter. On basis of dimensions, Nanomaterials are categorized as zero-dimensional, one dimensional, two-dimensional and three dimensional which are represented by 0D (Quantum dots), 1D (Nanorod), 2D (Nanosheet) and 3D (Nanoflowers) respectively [1]. The motion of electrons from conduction band and holes or excitons from valence band (bound pairs of conduction band electrons and valence band holes) are confined in all the three directions of a structure for quantum dots[2-4]. Since they were first identified in the 1980's, Semiconductor nanocrystals are also referred as Quantum Dots (QD's)[5-20]. A type of semiconductor nanocrystal known as Colloidal Quantum Dots has particle size smaller than the exciton Bohr radius of 5.4 nm for CdSe and their properties are dissimilar to those of bulk object due to few nanometers[21-26]. semiconductors QD's of II-VI group metal chalcogenides, especially ZnS, CdSe, and CdTe were extensively investigated due to their quantum confinement properties[27]. The quantum confinement effect occurs when the size of a particle is comparable to the electron's de Broglie wavelength. The hot injection method is a commonly used appach for synthesizing high-quality crystalline II-VI semiconductor materials. In this technique, a cadmium precursor like $(CH_3)_2Cd$ $(dimethylcadmium)$ or CdO $(Cadmium\ Oxide)$, is first dissolved in coordinating ligands, including trioctylphosphine oxide (TOPO), hexylphophonic acid or tetradecylphosphonic acid. The Se Precursor (Se dissolved in trioctylphosphine, TOP) is then rapidly introduced into the heated coordinating reaction mixture, triggering the nucleation process. The subsequent growth phase is performed at a comparatively lower temperature. This method was initially introduced by Murray et al. [28] and waws later refined and advanced by Peg et al. and Talapin et al. [29-36].

The synthesizing of CdSe QD's has been tried by numerous researchers using different techniques or by utilizing Cd and Se precursors. Lately, several methods have been tried to generate CdSe QD's: liquid paraffin with a combination[37], one-pot hydrothermal synthesis[38], microwave and electron beam irridation[39,40], colloidal reaction temperature technique[41], and aqueous solution[42-45]. In contrast to these methods, the synthesis

[1]Department of Physics, University of Mumbai, Vidyanagari Campus, Kalina, Santacruz (E), Mumbai 400 098, India.
[2]Department of Physics, Institute of Science,15, Madam Cama Road, Mantralaya, Fort, Mumbai 400 032, India.
Corresponding author Email: vaishali.bambole@physics.mu.ac.in

process that employ an aqueous solution have good water solubility and are easy, environmentally friendly, and highly reproducible.

When exposed to UV light, QDs with diameters of 5-6nm emit light at longer wavelengths, whereas those with smaller sizes, ranging from 2-3nm, emit light at shorter wavelengths and exhibit larger bandgaps. This behaviour arises because the electrons in QDs are confined to discrete energy levels, which are size-dependent, with smaller particles exhibiting larger bandgaps [46-47].

Hence, shorter wavelength means higher photon energy, which is required for Photovoltaic conversions. In this paper we are reporting to have synthesized CdSe QD's by the wet chemical method (colloidal method) in which water is used as a solvent, and the reaction happens at ambient temperature. The synthesis procedure is economic gives us very small quantum dot particles. Xray & SEM studies revealed interesting structural and morphological changes depending on temperature variation. highly pure form of CdSe QD's were obtained due to unique experimental setup. At temperature of 400C experiment of 5 hours small QD's of size 3.5nm were obtained. with the size of QD falling in the range of 3.5nm to 4nm and Bandgap of 2.60eV is obtained. So, we can claim that these quantum dots have the potential application in Photovoltaic and Dye-Sensitized solar cell.

II. MATERIALS AND METHODS:

A. Materials:

Cadmium Acetate Dihydrate [Cd $(CH3COO)_2$] (reagent grade, 98%, Aldrich), Selenium Metal Powder (Se) (100 mesh, 99.99% trace metals basis,Aldrich), 2-Merxaptoethanol ($HOCH_2CH_2SH$) (99%, SRL) also known as βME, Sodium Sulphite (Na_2SO_3) (Sodium Sulfite, ≥ 98%,Aldrich). All of the materials were employed without further purification because they were of analytical grade. Water as solvent had been twice distilled was used to produce each solution.

B. Synthesis of CdSe quantum dots:

Solution A as stock solution of Sodium Selenosulphite (Na_2SeSO_3) in two neck flasks was prepared by mixing of 0.6040 gm of Na_2SO_3 and 0.0948 gm of Se metal powder in 50ml of double distilled water (DDW). This solution was then heated at 90^0C for an hour. The second solution B was prepared by adding 0.46 gm of [Cd $(CH3COO)_2$ in 50ml of DDW at 40^0C for a period of 10 minutes. Solution A is then added to Solution B till the colourless solution B changes from Milky to dark lemon colour. Then 0.4ml of 2-Mercaptoethanol (βME) is added drop by drop till end of the experiment. A set of four experiment done at temperature 40^0C,55^0C,70^0C, and 85^0C for material T40^0C, T55^0C, T70^0C and T85^0C Respectively. Fig (1) showing pictorial graph of experiment.The Prepared Quantum dots were washed by Double Distilled Water for 3-4 times and keep it in Oven to dry the samples and convert it into the Powder.

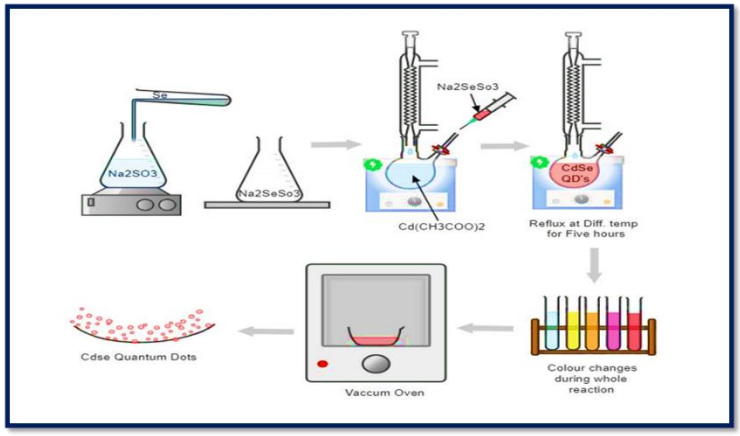

Fig. (1) Schematic illustration of the CdSe Colloidal Synthesis Process

III. RESULTS AND DISCUSSIONS:

A. Characterization and Evaluation:

An XPERT-PROMPD X-ray diffractometer with Cu-Kα radiation (λ = 1.5405 A0) in the range of (100 to 800) was applied for the identification of materials, crystal composition and Phase identification. JEOL-IT300 for scanning electron microscopy (SEM). For Absorbance study, the UV-Visible Spectrometer (Perkin-Elmer, Lambda 750) was used. Using a Perkin-Elmer 1710, the Fourier Transform Infrared (FTIR) spectra was acquired at a resolution of 2cm-1 across the 500-4000 cm-1 range. Using Thermo Scientific- Talos F200X G2, a High-resolution transmission electron microscopy (HRTEM) was used for atomic-scale imaging of a sample of crystalline structure. Energy-dispersive X-ray spectroscopy (EDS) was carried out to identify the chemical compositions and Selected Area Electron Diffraction (SAED) was used to determine the significant level of crystallinity in the porous material.

B. XRD Characterization:

The structure, composition and crystallite size analysis of the prepared CdSe QD's was performed using an XPERT-PROMD X-ray diffractometer (XRD) instrument recorded between the 2θ angles 20^0 to 60^0. The diffraction graph in the XRD shown in Figure (2). The standard [ICDD No. 19-191] [48,49] and [JCPDS No. 19-191] [50-60] have been three clear wide peaks could be identified at 2θ = 26.08°, 42.29°, 46.28° and 50.55° which corresponds to the lattice planes (111), (220) and (311). The formation of CdSe nanocrystalline structure is confirmed by peak broadening.

To calculate the crystallites size from Debye-Scherrer's formula,

$$D = \frac{K\lambda}{\beta \cos\theta} \qquad (1)$$

Where,

D = crystallites size (nm)

K = 0.9 (Scherrer's constant)

λ = 0.15406nm (wavelength of the x-ray sources)

β = FWHM (radians)

θ = Peak Position (radians)

To using the same, the estimate crystallite size was found out to be of CdSe QD's is 0.2 nm to 0.6 nm. Fig.(2) is the X-ray diffraction pattern of temperature of 40^0C,55^0C,70^0C, and 85^0C synthesized materials.

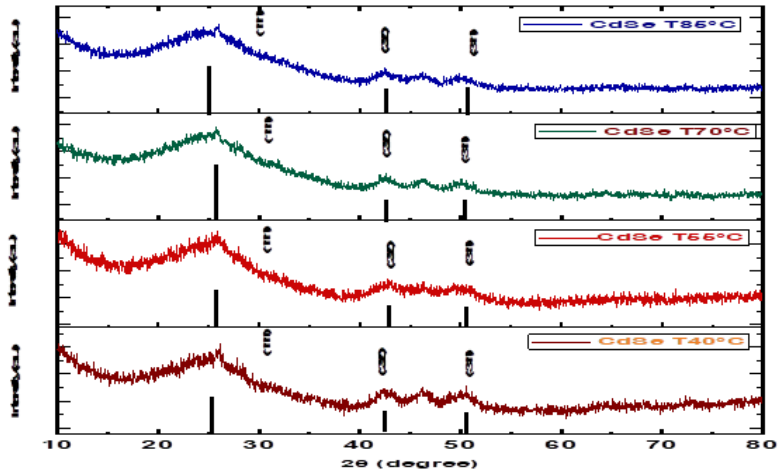

Fig (2): XRD pattern of CdSe QD's prepared at 40°C, 55°C, 70°C and 85°C

C. SEM Characterization:

Figure 3 illustrates the surface morphology of CdSe QDs synthesized at temperatures of $40℃, 55℃, 70℃, and\ 85℃$, corresponding to samples $T40℃, T55℃, T70℃, and\ T85℃$, respectively. The SEM images for these temperature series are depicted at $1000\times$ magnification in panels (a), (b), (c) and (d) and at $3000\times$ magnification in panels (e), (f), (g) and (h) for samples $T40℃, T55℃, T70℃, and\ T85℃$, respectively.

The particle size is being increases with increasing temperature. Also, Fig.3 is shows image of the uneven orientation of grains in the SEM image seems rough and agglomerated. It is preferable to trap charge carriers inside the gadget because of its rough construction, but doing so also reduces the device's responsiveness and mobility [61].

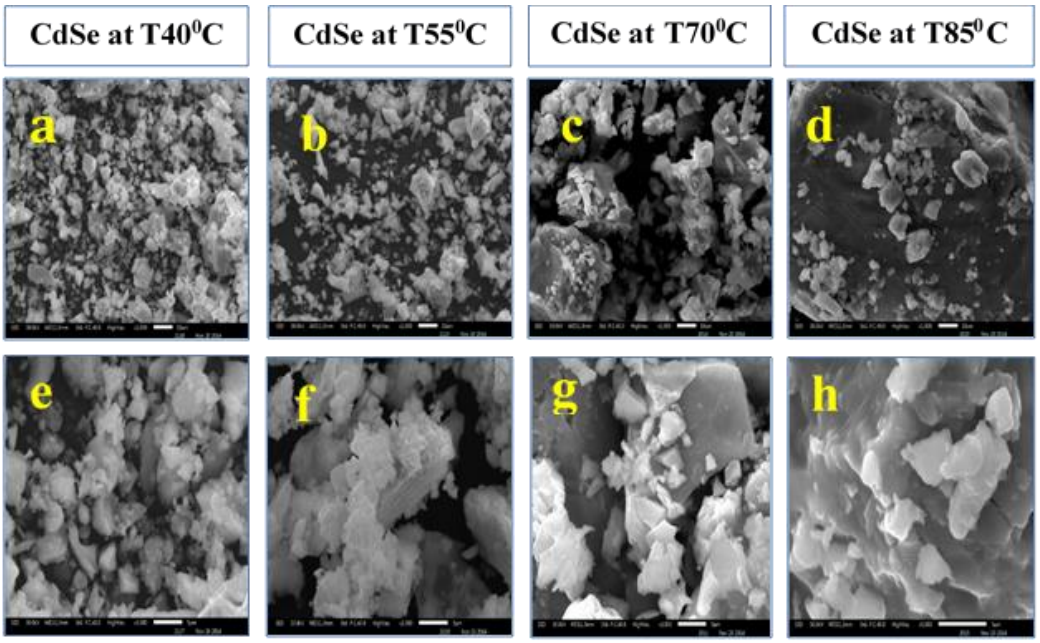

Fig. 3 (a-d) Temperature series of magnification rate 1000 and Fig. 3 (e-h) magnification rate 3000 for 40⁰C, 55⁰C, 70⁰C and 85⁰C of Samples T40⁰C, T55⁰C, T70⁰C and T85⁰C respectively

D. UV-Visible Spectroscopy:

Before being transferred into a quartz cuvette for analysis, a tiny portion of the powdered samples of T40^{0}C,T55^{0}C,T70^{0}C and T85^{0}C were sonicated in double distilled water to ensure appropriate dispersion. The UV-Vis absorption spectra confirms the red shift in colour implying increase in particle size [62-64]. The absorption spectra in Figure 3 shows how the particle size increases with temperature. Distinct peaks are observed at 595nm,619nm,599nm and 544nm with 40^{0}C,55^{0}C,70^{0}C and 85^{0}C respectively in all prepared CdSe QD's[65].

Bandgap determination:

The optical transition energy waws determined from the absorption spectra using Tauc's relation [2,62,66].

$$(\alpha h\upsilon) = B\,(h\upsilon - E_g)^r \qquad (2)$$

Where hν is the photon energy, E_g is the optical bandgap, B is a constant, and r is an index that realies on the type of electronic transition that results in optical absorption. The values of r for allowed direct, allowed indirect, forbidden direct and forbidden indirect transitions are 1/2, 2, 3/2, and 3, respectively. [21]

CdSe is recognized for its direct bandgap structure. For direct transitions, equation (1) is expressed as follows:

$$(\alpha h\nu) = B\,(h\nu - E_g)^{1/2} \qquad (3)$$

The relationship between$(\alpha h\nu)^2$ and $h\nu$ for synthesized CdSe QDs is depicted in the inset spectra of each group in Figure 3. The linearity observed across a wide photon energy range suggests a direct transition. The bandgap values ofr the samples prepared at $40℃, 55℃, 70℃, and\ 85℃$ were determined to be $2.60eV, 2.25eV, 2.08eV\ and\ 1.89eV$, respectively, which are higher than the bulk CdSe bandgap of $1.74eV$ [1, 21, 67]. The optical transition energy was determined by extrapolating the linear portion to the energy axis, where $(\alpha h\nu)^2 = 0$.

Fig.4(a), 4(b), 4(c) and 4(d) shows UV and Tauc graph of samples 40^0C,55^0C,70^0C and 85^0C respectively.

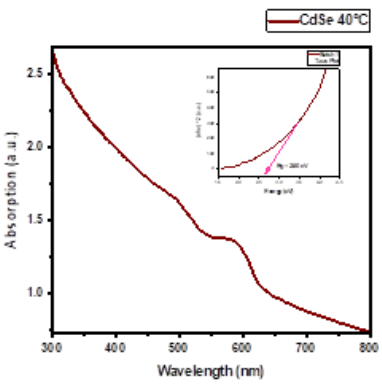

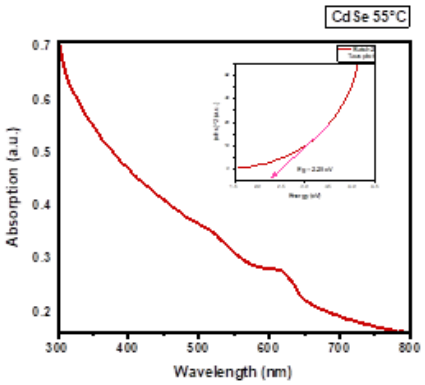

Fig. 4(a) UV and Tauc graph for samples T400C Fig. 4(b) UV and Tauc graph for samples T550C

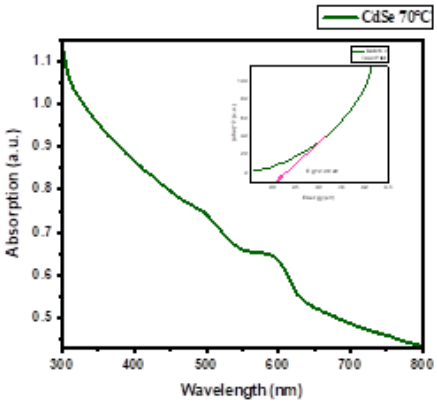

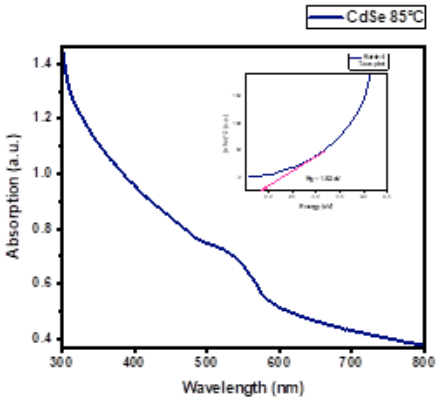

Fig. 4(c) UV and Tauc graph for samples T700C Fig. 4(d) UV and Tauc graph for samples T850C

E. FTIR Characterization:

The CdSe nonstructural material's organic species are identified and characterized by FTIR Spectroscopy. Figure 5 exhibits the FTIR analysis of CdSe QD's given below:

Sample No.	**Wavenumber as per Analysis (Cm-1)**	**Analysis**
T40^{0}C	735	Cd - Se band stretching [72]
	992	CH2 rocking [4]
	1281	CH2 wagging [4]
	2607	symmetric stretching vibration of C – CH2 from the methylene chain [72]
	3762	weak band [72]
	742	Cd - Se band stretching [72]

T55^{0}C	992	CH2 rocking [4]
	1289	CH2 wagging [54]
	1390	CH2 wagging [73]
	3279	O-H stretching of vibration peak [54]
	3435	the OH vibrations of hydroxyl group [74]
T70^{0}C	742	Cd - Se band stretching [72]
	1000	C-O stretching [73]
	1421	CH2 bending [73]
	3279	OH group [73]
	2849	Symmetric stretching in CH2 vibrations of alkyl chain [73]
T85^{0}C	633	C-S stretching [73]
	742	Cd - Se band stretching [72]
	992	CH2 rocking [4]
	1281	CH2 wagging [4]
	2888	Symmetric stretching in CH2 vibrations of alkyl chain [73]
	2943	Asymmetric stretching in CH2 vibrations of alkyl chain [73]

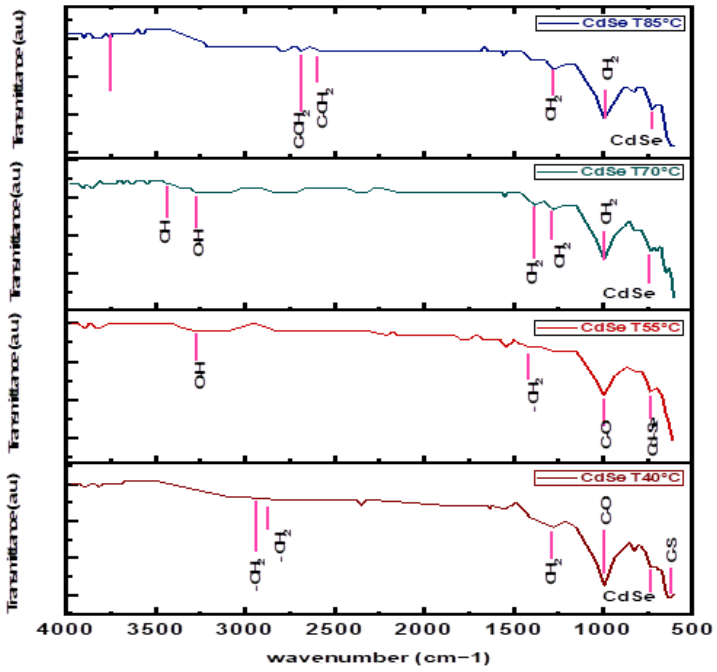

Fig. 5 FTIR Spectrum of the CdSe QD's

F. HR-TEM Characterization:

In Fig. 6(a) shows a HRTEM image of Samples T40^{0}C, in which several CdSe QD's are clearly visible and seen crystalline in nature. The average diameter was determined to be 3.65 nm. When compared to the size estimated from the XRD study, it was discovered that the quantum dots observed by HRTEM were slightly larger. The main reason of this result is due to the fact the X-ray only measures the nanocrystalline core size [68].

Figure 6(b) illustrates a histogram representing the size distribution of the measured QDs, with the majority having diameters ranging from 3.5nm to 4nm. Empirical relations proposed by Lu et al., which link size to excitonic peak position, suggest that the sizes and optical properties are in agreement [23,69-70,78-79]. HRTEM images of two QDs, along with their corresponding Fourier transformations, are presented in Figure 6(c) and 6(d).

The typical zig-zag pattern of the Wurtzite crystal structure appears by the Fourier transform in Fig. 6(c), and the QD's in Fig. 6(d) exhibit a Zinc blende crystal structure. The presence of CdSe QD's Quantum Yield (QY) increases as compared to the Wurtzite structure, Xia et al. hypothesized [69,71] that the Zinc blende structure in these particles leads to improved optoelectronic capabilities. The QDs displayed continuous lattie fringes consistent with the Wurtzite structure of CdSe, exhibiting an interplanar spacing of 0.385 *nm,* as observed in the HRTEM analysis in Figure 6(e). the lattice fringes are distinctly visible in the lower section of the same image.

Intensity Profile obtained from the atomic coloumn distance with lines in (e), with help of graph in Fig. 6(f) we have calculated the Interplanar Spacing in Fig. 6(e).

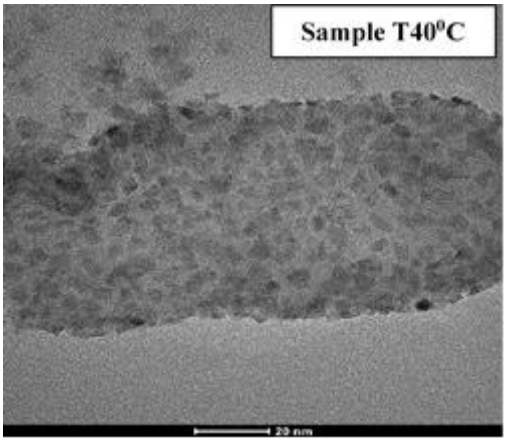

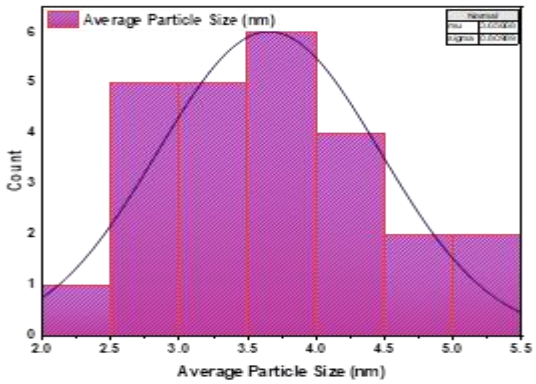

Fig. 6(a) HRTEM of CdSe QD's Fig. 6 (b) Histogram of CdSe QD's

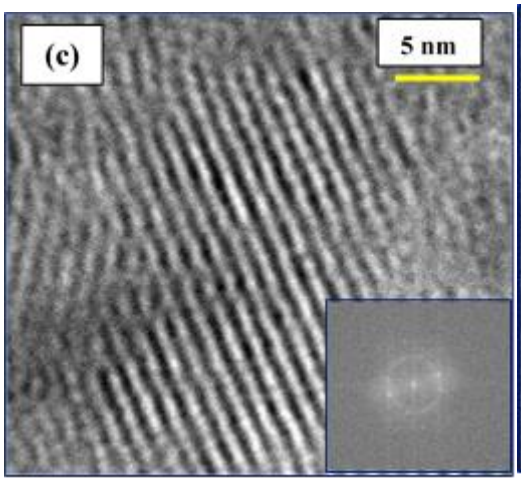

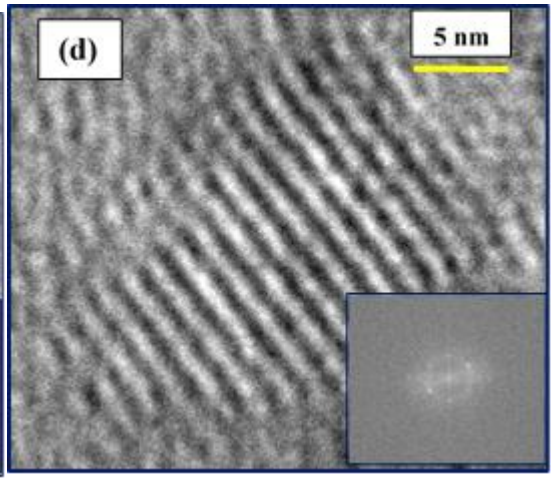

Fig. 6 (c) CdSe QD's with Wurtzite Structure Fig. 6 (d) CdSe QD's with Zinc Blende Structure

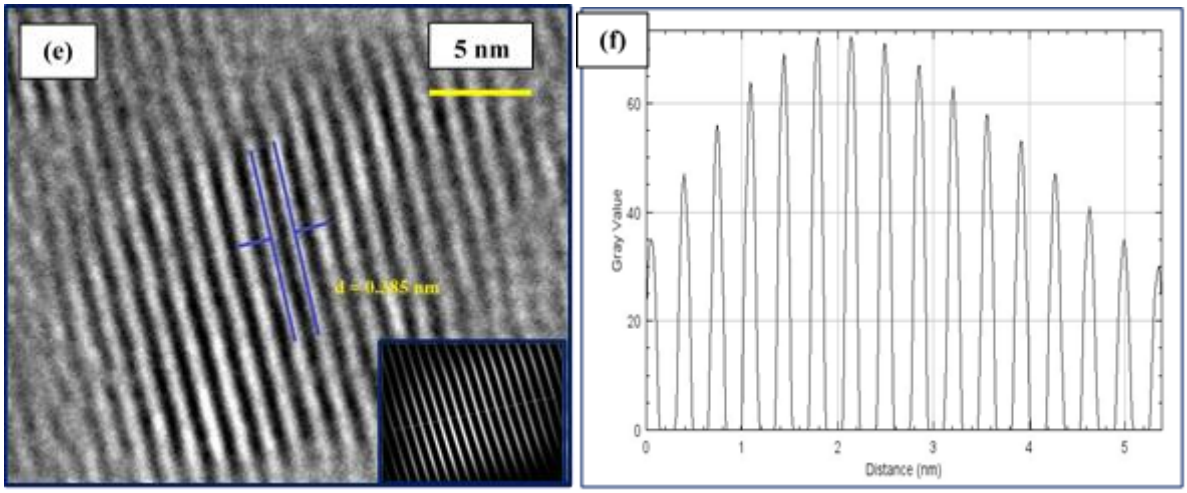

Fig. 6 (e) Interplanar Spacing of CdSe QD's Fig. 6 (f) The intensity profiles, derived from the atomic columns indicated by the lines in panel 6(e), were analyzed with respect to the interplanar spacing.

G. EDX Characterization:

In order to confirm the formation of CdSe QD's EDX analysis was performed. During the EDX measurement different areas were focused and the corresponding peaks are shown in Fig. 7. Both Cd and Se can be seen in the synthesized QD's in the EDX Spectrum. In Spectrum, the atomic quantity of Cd and Se were 76.03 and 23.96 respectively.

Details of the EDX Spectra of the CdSe QD's values measured as atomic and weight % are listed in Table 7 (i):

Element	**Cadmium (Cd)L**		**Selenium (Se)K**	
	Weight(%)	**Atomic (%)**	**Weight (%)**	**Atomic (%)**
CdSe QD's	81.87	76.03	18.12	23.96

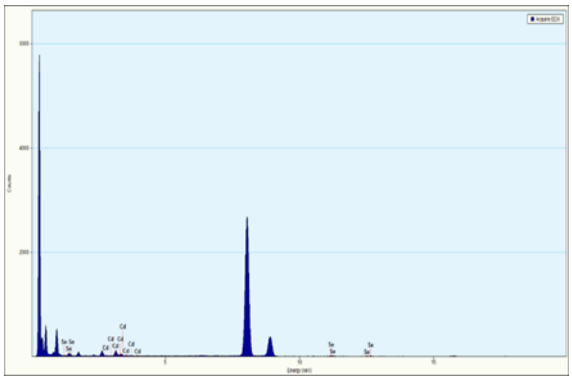

Fig.7(i) EDX Spectra of CdSe QD's

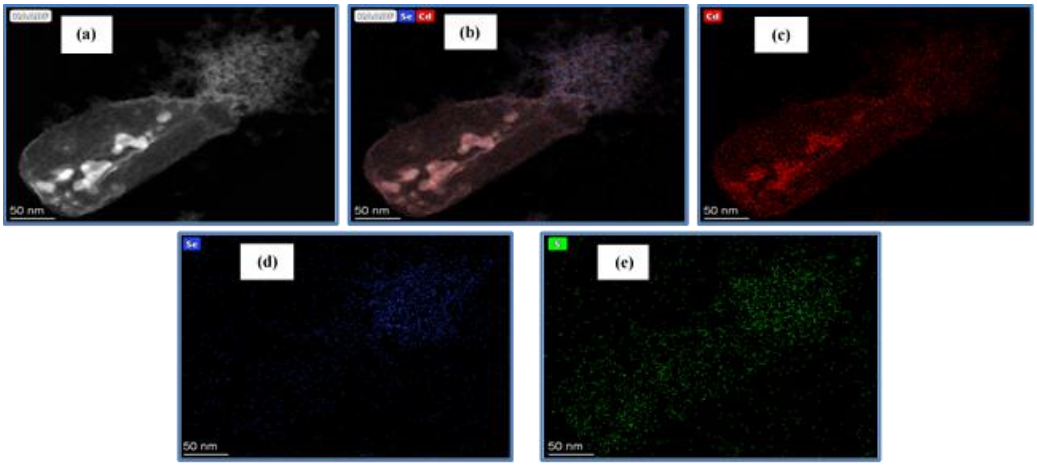

Fig. 7 Element distribution maps of CdSe QD's. (a-b) HAADF-STEM image, (c–e) positions of Cd, Se, and S atoms respectively.

Energy dispersion X-ray (EDX) Spectroscopy was used to generate element distribution maps in order to investigate the locations of Cd, Se, and S in CdSe QD's (Figure 7). Using Scanning transmission electron microscopy (STEM), a high angle annular dark field (HAADF) [23,78,79,80, 81] image of the sample CdSe QD's is displayed in Figure 7(a). The distribution of the Cd and Se elements in the same picture is shown in Figure 7(b). The positions of the atoms of Cd, Se, and S are shown in Figure 7(c-e). The intensity of the K (Se) or L (Cd) line in the EDX spectrum determines the colour brightness of a single selected pixel [23]. Element Cd distributed more in the lower half side as compared to the upper part of the structure in Fig. 7(c), Element Se distributed more in top right part of the structure in Fig.7 (d) and Element S is evenly distributed throughout the entire structure in Fig.7 (e).

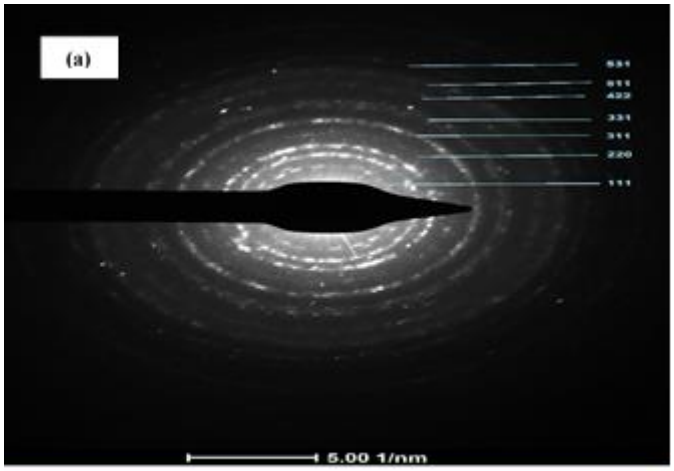

Fig.8 (a) Selected Area Electron Diffraction (SAED)

H. *SAED Characterization:*

The SAED of the T40^{0}C sample is displayed in Figure 8(a);The Sample's good crystallinity is indicated by the presence of distinct diffraction rings. The lattice planes that emerged had smaller interplanar spacing(d) than the bulk and were indexed with cubic planes (111), (220), (311), (422), (511) and (531). Thses lattice planes are Polycrystalline clear diffraction rings structure associated with the CdSe QD's is cubic. [4,54, 68, 75, 76]. That XRD data by confirming that the Samples main phase has a Modified cubic structure.The polycrystalline clear diffraction rings structure of the produced CdSe nanoparticles' SAED pattern correlates to the lattice planes (111), (220), and (311), respectively, and is associated with cubic CdSe nanoparticles.

IV. Conclusion

Using the wet chemical method, CdSe QD's are synthesized. XRD results reveal 0.2nm to 0.6nm particle size, at temperature 40^{0}C showing cubic phase with zinc blend structure of CdSe QD's. SEM morphology shows that the

particle size increase with increasing temperature and the band gap decreases from 2.60 eV to 1.89 eV for temperature 40^0C,55^0C,70^0C and 85^0C respectively. Among all-material that we studied, the average particle size 3.65nm and the smallest particle size is 1nm as well as the Wurtzite crystal structure and Zinc blende crystal structure appears by the Fourier Transform of material of temperature 40^0C. The surface area increases as the particle size decreases [82]. These CdSe QD's did not agglomerate even after 550 days without using any Stabilizing agent. The typical zig-zag pattern of the Wurtzite crystal structure of CdSe QD's can be also confirmed by Fast Fourier Transform (FFT) which is a generalized through ImageJ plug in for the calculation of Fourier transform. In Fig. 6(c), and the QD's in Fig. 6(d) exhibit a zinc blende crystal structure.

With these results, we conclude that with temperature set at 40^0C is promising material for the Dye Sensitized Solar Cell application.

V. Acknowledgement

The authors extend their sincere gratitude to Government of Maharashtra's ISMAIL YUSUF COLLEGE of Arts, Science & Commerce, Mumbai, India for helping in FTIR, and Indian Institute of Technology Dhanbad, Jharkhand, India for helping with fine results of HRTEM.

References

[1] Ameta, S.C., 2022. Nanomaterials: An Introduction. In The Science of Nanomaterials (pp. 1-18). Apple Academic Press.

[2] Karan Surana, Pramod K Singh, Hee-Woo Rhee, B. Bhattacharya, "Synthesis, characterization and application of CdSe quantum dots", Journal of Industrial and Engineering Chemistry, Volume 20, Issue 6, Pages 4188-4193, 25 November 2014.

[3] Karan Surana , Ibrahim T. Salisu , R.M. Mehra , Bhaskar Bhattacharya, "A simple synthesis route of low temperature CdSe-CdS core-shell quantum dots and its application in solar cell", Optical Materials, Volume 82, Pages 135-140, August 2018.

[4] Mahesh Verma, D. Patidar, K. B. Sharma, and N. S. Saxena, "Synthesis, Characterization and Optical Properties of CdSe and ZnSe Quantum Dots", Journal of Nanoelectronics and Optoelectronics Vol. 10, 1–7, 2015.

[5] Ekimov, A.I. and Onushchenko, A.A., 1982. Quantum size effect in the optical-spectra of semiconductor micro-crystals. Sov. Phys. Semicond, 16(7), pp.775-778.

[6] Brus, L.E., 1984. Electron–electron and electron-hole interactions in small semiconductor crystallites: The size dependence of the lowest excited electronic state. The Journal of chemical physics, 80(9), pp.4403-4409.

[7] Zhang, M., Bishop, B.P., Thompson, N.L., Hildahl, K., Dang, B., Mironchuk, O., Chen, N., Aoki, R., Holmberg, V.C. and Nance, E., 2019. Quantum dot cellular uptake and toxicity in the developing brain: Implications for use as imaging probes. Nanoscale advances, 1(9), pp.3424-3442.

[8] Tang, X., Ackerman, M.M., Chen, M. and Guyot-Sionnest, P., 2019. Dual-band infrared imaging using stacked colloidal quantum dot photodiodes. Nature photonics, 13(4), pp.277-282.

[9] Moon, H., Lee, C., Lee, W., Kim, J. and Chae, H., 2019. Stability of quantum dots, quantum dot films, and quantum dot light-emitting diodes for display applications. Advanced Materials, 31(34), p.1804294.

[10] Chen, K.; Zhong, Q.; Chen, W.; Sang, B.; Wang, Y.; Yang, T.; Liu, Y.; Zhang, Y.; Zhang, H. Short-Chain Ligand-Passivated Stable α-CsPbI3 Quantum Dot for All-Inorganic Perovskite Solar Cells. Adv. Funct. Mater. 2019, 29, 1900991.

[11] Yan, D.; Shi, T.; Zang, Z.; Zhou, T.; Liu, Z.; Zhang, Z.; Du, J.; Leng, Y.; Tang, X. Ultrastable CsPbBr3 Perovskite Quantum Dot and Their Enhanced Amplified Spontaneous Emission by Surface Ligand Modification. Small 2019, 15, 1901173.

[12] Song, J.; Wang, O.; Shen, H.; Lin, Q.; Li, Z.; Wang, L.; Zhang, X.; Song, L. Over 30% External Quantum Efficiency Light-Emitting Diodes by Engineering Quantum Dot-Assisted Energy Level Match for Hole Transport. Layer Adv. Funct. Mater. 2019, 29, 1808377.

[13] Ma, F.; Zhang, Q.; Zhang, C. Catalytic Self-Assembly of Quantum-Dot-Based MicroRNA Nanosensor Directed by Toehold-Mediated Strand Displacement Cascade. Nano Lett. 2019, 19, 6370–6376.

[14] Shi, L.; Meng, L.; Jiang, F.; Ge, Y.; Li, F.; Wu, X.-G.; Zhong, H. In Situ Inkjet Printing Strategy for Fabricating Perovskite Quantum Dot Patterns. Adv. Funct. Mater. 2019, 29, 1903648.

[15] Zhang, H.; Hu, N.; Zeng, Z.; Lin, Q.; Zhang, F.; Tang, A.; Jia, Y.; Li, L.S.; Shen, H.; Teng, F.; et al. High-Efficiency Green InP Quantum Dot-Based Electroluminescent Device Comprising Thick-Shell Quantum Dots. Adv. Optical Mater. 2019, 7, 1801602.

[16] Yuan, J.; Bi, C.; Wang, S.; Guo, R.; Shen, T.; Zhang, L.; Tian, J. Spray-Coated Colloidal Perovskite Quantum Dot Films for Highly Efficient Solar Cells. Adv. Funct. Mater. 2019, 29, 1906615.

[17] Chebrolu, V.T.; Kim, H.-J. Recent progress in quantum dot sensitized solar cells: An inclusive review of photoanode, sensitizer, electrolyte, and the counter electrode. J. Mater. Chem. C 2019, 7, 4911–4933.
[18] Li, X.; Lin, Q.; Song, J.; Shen, H.; Zhang, H.; Li, L.S.; Li, X.; Du, Z. Quantum-Dot Light-Emitting Diodes for Outdoor Displays with High Stability at High Brightness. Adv. Opt. Mater. 2020, 8, 1901145.
[19] Sun, Y.; Su, Q.; Zhang, H.; Wang, F.; Zhang, S.; Chen, S. Investigation on Thermally Induced Efficiency Roll-Off: Toward Efficient and Ultrabright Quantum-Dot Light-Emitting Diodes. ACS Nano 2019, 13, 11433–11442.
[20] Ouellette, O.; Lesage-Landry, A.; Scheffel, B.; Hoogland, S.; de Pelayo García Arquer, F.; Sargent, E.H. Spatial Collection in Colloidal Quantum Dot Solar Cells. Adv. Funct. Mater. 2020, 30, 1908200.
[21] Waleed E. Mahmoud, Amal M. Al-Amri, S.J. Yaghmour, "Low temperature synthesis of CdSe capped 2-mercaptoethanol quantum dots", Optical Materials, Volume 34, Issue 7, Pages 1082-1086, May 2012.
[22] Yukun Gao and PG Yin, "Synthesis of cubic CdSe nanocrystals and their spectral properties", Nanomaterials and Nanotechnology Volume 7: 1–6 The Author(s) 2017.
[23] Kotin, P.A., Bubenov, S.S., Mordvinova, N.E. and Dorofeev, S.G., 2017. AgCl-doped CdSe quantum dots with near-IR photoluminescence. Beilstein Journal of Nanotechnology, 8(1), pp.1156-1166.
[24] Alivisatos, A.P., 1996. Semiconductor clusters, nanocrystals, and quantum dots. science, 271(5251), pp.933-937.
[25] Hoy, J., Morrison, P.J., Steinberg, L.K., Buhro, W.E. and Loomis, R.A., 2013. Excitation energy dependence of the photoluminescence quantum yields of core and core/shell quantum dots. The Journal of Physical Chemistry Letters, 4(12), pp.2053-2060.
[26] Luther, J.M. and Pietryga, J.M., 2013. Stoichiometry control in quantum dots: a viable analog to impurity doping of bulk materials. ACS nano, 7(3), pp.1845-1849.
[27] Ramalingam, G., Ragupathi, C., Kaviyarasu, K., Letsholathebe, D., Mohamed, S.B., Magdalane, C.M., Mola, G.T., Isaev, A.B. and Maaza, M., 2019. Up-scalable synthesis of size-controlled white-green emitting behavior of core/shell (CdSe/ZnS) quantum dots for LED applications. Journal of nanoscience and nanotechnology, 19(7), pp.4026-4032.
[28] Cingarapu, S., Yang, Z., Sorensen, C.M. and Klabunde, K.J., 2012. Synthesis of CdSe/ZnS and CdTe/ZnS quantum dots: refined digestive ripening. Journal of Nanomaterials, 2012, pp.7-7.
[29] D. Battaglia, J. J. Li, Y. Wang, and X. Peng, "Colloidal twodimensional systems: CdSe quantum shells and wells," Angewandte Chemie—International Edition, vol. 42, no. 41, pp. 5035–5039, 2003.
[30] X. Peng, L. Manna, W. Yang et al., "Shape control of CdSe nanocrystals," Nature, vol. 404, no. 6773, pp. 59–61, 2000.
[31] Z. A. Peng and X. Peng, "Formation of high-quality CdTe, CdSe, and CdS nanocrystals using CdO as precursor," Journal of the American Chemical Society, vol. 123, no. 1, pp. 183–184, 2001.
[32] L. Qu, Z. A. Peng, and X. Peng, "Alternative routes toward high quality CdSe nanocrystals," Nano Letters, vol. 1, no. 6, pp. 333– 337, 2001.
[33] D. V. Talapin, A. L. Rogach, A. Kornowski, M. Haase, and H. Weller, "Highly luminescent monodisperse CdSe and CdSe/ZnS nanocrystals synthesized in a hexadecylamine-trioctylphosphine oxide-trioctylphospine mixture," Nano Letters, vol. 1, no. 4, pp. 207–211, 2001.
[34] H. Yang, N. Fan, W. Luan, and S. T. Tu, "Synthesis of monodisperse nanocrystals via microreaction: open-to-air synthesis with oleylamine as a coligand," Nanoscale Research Letters, vol. 4, no. 4, pp. 344–352, 2009.
[35] W. W. Yu and X. Peng, "Formation of high-quality CdS and other II–VI semiconductor nanocrystals in noncoordinating solvents: tunable reactivity of monomers," Angewandte Chemie—International Edition, vol. 41, no. 13, pp. 2368–2371, 2002.
[36] Cingarapu, S., Yang, Z., Sorensen, C.M. and Klabunde, K.J., 2012. Synthesis of CdSe/ZnS and CdTe/ZnS quantum dots: refined digestive ripening. Journal of Nanomaterials, 2012, pp.7-7.
[37] Liu J., Gu S., Pan K., ET AL.: 'Synthesis and photoluminescence properties of high–quality CdSe quantum dot in liquid paraffin', Micro Nano Lett., 2011, 6, (11), pp. 964–966
[38] Song X., Liu X., Yan Y., ET AL.: 'One–pot hydrothermal synthesis of thioglycolic acid-capped CdSe quantum dots-sensitized mesoscopic TiO2 photoanodes for sensitized solar cells', Sol. Energy Maters. Sol. Cells, 2018, 176, pp. 418–426
[39] Zhang T., Jin J., Yang C., ET AL.: 'Microwave synthesis CdSe quantum dot clusters via ribonuclease a protein', Micro Nano Lett., 2012, 7, (12), pp. 1289–1291
[40] Singh A., Tripathi V.S., Neogy S., ET AL.: 'Facile and green synthesis of l-thioglycerol capped CdSe quantum dots in aqueous solution', Mater. Chem. Phys., 2018, 214, pp. 320–329
[41] Bhand G.R., Lakhe M.G., Rohom A.B., ET AL.: 'Synthesis and characterization of controlled size CdSe quantum dots by colloidal method', J. Nanosci. Nanotechnol., 2018, 18, (4), pp. 2695–2701
[42] Singh A., Guleria A., Kunwar A., ET AL.: 'Saccharide capped CdSe quantum dots grown via electron beam irradiation', Mater. Chem. Phys., 2017, 199, pp. 609–615
[43] Wang Y., Yang K., Pan H., ET AL.: 'Synthesis of high–quality CdSe quantum dots in aqueous solution', Micro Nano Lett., 2012, 7, (9), pp. 889–891

[44] Lan Y., Yang K., Wang Y., ET AL.: 'Aqueous synthesis of highly luminescent CdSe quantum dots with narrow spectra using hydrazine hydrate reduction selenium', Micro Nano Lett., 2014, 9, (3), pp. 202–205
[45] Akter, M., Khan, M.N.I., Mamur, H. and Bhuiyan, M.R.A., 2020. Synthesis and characterisation of CdSe QDs by using a chemical solution route. Micro & Nano Letters, 15(5), pp.287-290.
[46] Brus, L.E. Electron-Electron and electron-hole interactions in small semiconductor crystallites: The size dependence of the lowest excited electronic state. J. Chem. Phys. 1984, 80, 4403–4409.
[47] Sanmartín-Matalobos, J., Bermejo-Barrera, P., Aboal-Somoza, M., Fondo, M., García-Deibe, A.M., Corredoira-Vázquez, J. and Alves-Iglesias, Y., 2022. Semiconductor Quantum Dots as Target Analytes: Properties, Surface Chemistry and Detection. Nanomaterials, 12(14), p.2501.
[48] Avinash Singh, Amit Kunwar, and M. C. Rath, "L-Cysteine Capped CdSe Quantum Dots Synthesized by Photochemical Route", Journal of Nanoscience and Nanotechnology Vol. 17, 1–8, 2017
[49] Zainab H. Omran, Odai N. Salman* and A. K. Ali, "Preparation CdSe Quantum Dots using laser ablation technique for Dye-Sensitized Solar Cell", International Journal of Nanoelectronics & Materials. Vol. 14 Issue 1, p61-69. 9p, Jan2021.
[50] Waleed E. Mahmoud, Amal M. Al-Amri, S.J. Yaghmour, "Low temperature synthesis of CdSe capped 2-mercaptoethanol quantum dots", Optical Materials, Volume 34, Issue 7, Pages 1082-1086, May 2012.
[51] Mahesh Verma, D. Patidar, K. B. Sharma, and N. S. Saxena, "Synthesis, Characterization and Optical Properties of CdSe and ZnSe Quantum Dots", Journal of Nanoelectronics and Optoelectronics Vol. 10, 1–7, 2015.
[52] Kale, R.B. and Lokhande, C.D., 2004. Band gap shift, structural characterization and phase transformation of CdSe thin films from nanocrystalline cubic to nanorod hexagonal on air annealing. Semiconductor science and technology, 20(1), p.1.
[53] Kale, R.B. and Lu, S.Y., 2015. Air annealing induced transformation of cubic CdSe microspheres into hexagonal nanorods and micro-pyramids. Journal of Alloys and Compounds, 640, pp.504-510.
[54] Jamble, S.N., Ghoderao, K.P. and Kale, R.B., 2017. Hydrothermal assisted growth of CdSe nanoparticles and study on its dielectric properties. Materials Research Express, 4(11), p.115029.
[55] Raut, V.S., Lokhande, C.D. and Killedar, V.V., 2017. Studies on effect of pH on structural, optical and morphological properties of chemisynthesized CdSe grains. International Journal of Engineering, 10(1), p.2017.
[56] Hodlur, R.M. and Rabinal, M.K., 2014. A new selenium precursor for the aqueous synthesis of luminescent CdSe quantum dots. Chemical Engineering Journal, 244, pp.82-88.
[57] Kim, J., Choi, S., Noh, J., Yoon, S., Lee, S., Noh, T., Frank, A.J. and Hong, K., 2009. Synthesis of CdSe− TiO2 nanocomposites and their applications to TiO2 sensitized solar cells. Langmuir, 25(9), pp.5348-5351.
[58] Akter, M., Khan, M.N.I., Mamur, H. and Bhuiyan, M.R.A., 2020. Synthesis and characterisation of CdSe QDs by using a chemical solution route. Micro & Nano Letters, 15(5), pp.287-290.
[59] Kumar Gupta D., Verma M., Patidar D., ET AL.: 'Synthesis, characterization and optical properties of CdSe and ZnSe quantum dots', Nanosci. Nanotechnol.–Asia, 2017, 7, (1), pp. 73–79
[60] Masteri-Farahani M., Mollatayefeh N.: 'Chiral colloidal CdSe quantum dots functionalized with cysteine molecules: new optical nanosensor for selective detection and measurement of morphine', Colloids Surf. A, Physicochem. Eng. Aspects, 2019, 569, pp. 78–84
[61] Wang, Q. and Seo, D.K., 2006. Synthesis of deep-red-emitting CdSe quantum dots and general non-inverse-square behavior of quantum confinement in CdSe quantum dots. Chemistry of Materials, 18(24), pp.5764-5767.
[62] Waleed E. Mahmoud, Amal M. Al-Amri, S.J. Yaghmour, "Low temperature synthesis of CdSe capped 2-mercaptoethanol quantum dots", Optical Materials, Volume 34, Issue 7, Pages 1082-1086, May 2012.
[63] Waleed E. Mahmoud, A.A. Al-Ghamdi, F. El-Tantawy, S. Al-Heniti, J. Alloys Compd. 485 (2009) 59.
[64] Waleed E. Mahmoud, J. Cryst. Growth 312 (2010) 3075.
[65] Karan Surana, R.M. Mehra, B. Bhattacharya, "Quantum Dot Solar Cells with size tuned CdSe QDs exhibiting 1.51V", Materials Today: Proceedings 5, Volume 5, Issue 3, Part 1, Pages 9108-9113, 2018.
[66] J. Tauc, Amorphous and Liquid Semiconductors, Plenum Press, New York, NY, 281 1974. 282.
[67] Waleed E. Mahmoud, H.M. El-Mallah, J. Phys. D: Appl. Phys. 42 (2009) 035502.
[68] Wageh, S., Al-Ghamdi, A., Jilani, A. and Iqbal, J., 2018. Facile Synthesis of Ternary Alloy of CdSe1-x S x Quantum Dots with Tunable Absorption and Emission of Visible Light. Nanomaterials, 8(12), p.979.
[69] Fernández-Delgado, N., Herrera, M., Tavabi, A.H., Luysberg, M., Dunin-Borkowski, R.E., Rodriguez-Cantó, P.J., Abargues, R., Martínez-Pastor, J.P. and Molina, S.I., 2018. Structural and chemical characterization of CdSe-ZnS core-shell quantum dots. Applied Surface Science, 457, pp.93-97.
[70] W.W. Yu, L. Qu, W. Guo, X. Peng, Experimental determination of the extinction coefficient of CdTe, CdSe, and CdS nanocrystals, Chem. Mater. 15 (2003) 2854–2860.
[71] X. Xia, Z. Liu, G. Du, Y. Li, M. Ma, Wurtzite and zinc-blende CdSe based core/shellsemiconductor nanocrystals: Structure, morphology and photoluminescence, J.Lumin. 130 (2010) 1285–1291.
[72] P Sanjay , K Deepa, J Madhavan and S Senthil, "Synthesis and Spectroscopic Characterization of Cdse Nanoparticles for Photovoltaic Applications", IOP Conf. Series: Materials Science and Engineering 360,012010,(2018).

[73] G. Ramalingam, K. Venkata Saravanan, T. Kayal Vizhi, M. Rajkumar and Kathirvelu Baskar, "Synthesis of water-soluble and bio-taggable CdSe@ZnS quantum dots", RSC Adv., 8, 8516, 2018.

[74] S. Reghuram, A. Arivarasan , R. Kalpana * and R. Jayavel, "CdSe and CdSe/ZnSquantum dots for the detection of C-reactive protein", Journal of Experimental Nanoscience ,Volume 10, Issue 10, 2015

[75] Kale, R.B. and Lokhande, C.D., 2005. Systematic study on structural phase behavior of CdSe thin films. The Journal of Physical Chemistry B, 109(43), pp.20288-20294.

[76] Nor Aliya Hamizi* , Mohd Rafie Johan, "Enhanced Ripening Behaviour of Cadmium Selenide Quantum Dots (CdSe QDs)", Int. J. Electrochem. Sci., 7 8473 – 8480, (2012).

[77] E.A. Larios-Rodríguez, F.F. Castillón-Barraza, R. Herrera-Urbina, U. Santiago, A. Posada-Amarillas, Synthesis of aucorepdshell nanoparticles by a green chemistry method and characterization by HAADF-STEM imaging, J. Clust. Sci. 28 (2017) 2075–2086

[78] D.S. He, Z.Y. Li, J. Yuan, Kinematic HAADF-STEM image simulation of small nanoparticles, Micron 74 (2015) 47–53

[79] N. Fernandez-Delgado, M. Herrera, J. Pizarro, P. Galindo, S.I. Molina, HAADF-STEM for the analysis of core-shell Quantum Dots, J. Mater. Sci. (2018).

[80] Held, J.T., Hunter, K.I., Dahod, N., Greenberg, B., Reifsnyder Hickey, D., Tisdale, W.A., Kortshagen, U. and Mkhoyan, K.A., 2018. Obtaining Structural Parameters from STEM–EDX Maps of Core/Shell Nanocrystals for Optoelectronics. ACS Applied Nano Materials, 1(2), pp.989-996.

[81] Weigert, F., Müller, A., Häusler, I., Geißler, D., Skroblin, D., Krumrey, M., Unger, W., Radnik, J. and Resch-Genger, U., 2020. Combining HR-TEM and XPS to elucidate the core–shell structure of ultrabright CdSe/CdS semiconductor quantum dots. Scientific reports, 10(1), p.20712.

[82] Alshora, D.H., Ibrahim, M.A. and Alanazi, F.K., 2016. Nanotechnology from particle size reduction to enhancing aqueous solubility. In Surface chemistry of nanobiomaterials (pp. 163-191). William Andrew Publishing.